

Short Communication

Monodisperse Liquid-filled Biodegradable Microcapsules

Cory Berkland,^{3,6} Emily Pollauf,⁵ Neel Varde,¹ Daniel W. Pack,¹ and Kyekyoon (Kevin) Kim^{2,4,6}

Received August 25, 2006; accepted November 28, 2006; published online March 20, 2007

Purpose. Encapsulation of liquids into biodegradable polymer microcapsules has been a challenging task due to production limitations stemming from solution viscosity, phase stabilization, molecular localization, and scalable production. We report an extension of Precision Particle Fabrication (PPF) technology for the production of monodisperse liquid-filled microcapsules containing an oil or aqueous core and contrast these results to double-walled microspheres.

Materials and Methods. PPF technology utilizes a coaxial nozzle to produce a liquid core jet surrounded by a polymer annular jet, which is further encompassed by a non-solvent carrier stream, typically 0.5% wt/vol polyvinyl alcohol in water. Jet diameters are controlled by the volumetric flow rate of each phase. The compound jet is then disrupted into uniform core/shell droplets via a controllable acoustic wave and shell material is hardened by solvent extraction.

Results. Monodisperse polymeric microcapsules demonstrated a narrow size distribution and the formation of a continuous shell leading to efficient encapsulation of various liquid cores. The intermingling of core and shell phases and the localization of different molecular probes (fluorescent dyes and fluorescently labeled proteins) to the core or shell phase provided additional evidence of phase separation and molecular partitioning, respectively. We also demonstrate the pulsatile release of bovine serum albumin encapsulated in an aqueous core.

Conclusions. PPF technology provided exceptional control of the overall size and shell thickness of microcapsules filled with various types of oil or water. This technique may enable advanced delivery profiles of pharmaceuticals or nutraceuticals.

KEY WORDS: controlled release; drug delivery; microcapsule; monodisperse; poly(lactide-co-glycolide).

INTRODUCTION

Recent advances in technology at the micro- and nanometer scale have yielded remarkable control over particle size and morphology. Precisely engineered particles are impacting areas such as drug delivery (1–4), photonics (5), cell encapsulation (6), and catalysis (7). Emerging techniques for creating monodisperse microspheres utilize controlled flow fields (8,9) and electrohydrodynamic forces (5,10,11) to induce regular droplet break-up. Although powerful, such techniques often possess limited production rates and typically require additional processing steps if a

coating material is desirable to enhance particle performance. Layer by layer coating (12) or colloidal assembly (7,13) at the surface of a core microsphere may provide an acceptable alternative to Wurster coating techniques for generating a coating layer, but possess limitations when generating thick coatings or encapsulating a liquid core. Here we report one-step Precision Particle Fabrication (PPF) of monodisperse polymeric microcapsules encapsulating an oil or aqueous core in comparison to double-walled (polymer core/polymer shell) microcapsules. Molecules are localized to the core or shell phase to enable advanced controlled release profiles, including pulsatile drug delivery.

Previously, we reported a Precision Particle Fabrication (PPF) technology capable of generating monodisperse microspheres and double-walled microspheres in a single step wherein 95% of the particle population exists within $\sim 1 \mu\text{m}$ of the average diameter for particle sizes from ~ 1 to $>500 \mu\text{m}$ (14–19). Production rates using PPF exceed 50 mg/min for a single nozzle ($50 \mu\text{m}$ particle), which we have scaled to $>1 \text{ kg/min}$ by using an array of nozzles. The production of double-walled microspheres required careful selection of solvent, polymer, and polymer concentration to encourage droplet phase separation into a core/shell structure. Biodegradable liquid-core microcapsules suitable as injectable drug delivery systems (~ 10 – $150 \mu\text{m}$) also require careful consideration of

¹ Department of Chemical and Biomolecular Engineering, University of Illinois, Urbana, Illinois 61801, USA.

² Department of Electrical and Computer Engineering, University of Illinois, Urbana, Illinois 61801, USA.

³ Department of Chemical and Petroleum Engineering, Department of Pharmaceutical Chemistry, 2030 Becker Dr., Lawrence, Kansas 66047, USA.

⁴ 45 Everitt Laboratory, 1406 West Green Street, Urbana, Illinois 61801, USA.

⁵ Chemical and Biological Engineering, College of Engineering & Applied Science, 424 UCB Boulder, Colorado, 80309-0424, USA.

⁶ To whom correspondence should be addressed. (e-mail: berkland@ku.edu; kevinkim@uiuc.edu)

interfacial tension, spreading coefficients, osmotic pressure, solvent extraction kinetics, etc. to generate a singlet core encapsulated in a uniform polymeric shell.

Monodisperse microcapsules were produced from various material combinations by utilizing three coaxial nozzles to generate a core jet and annular dissolved-polymer jet surrounded by a carrier stream (Fig. 1) (16,20–22). Volumetric flow-rates are controlled to modulate the diameters of jets emerging from the nozzle assembly. Nozzles possessed orifices from 100 to 500 μm in diameter, most typically $\sim 250 \mu\text{m}$. Typical, volumetric flow-rates for core, annular, and carrier jets were in the range of 1–50 mL/hr, 10–200 mL/hr, and 1–10 mL/min, respectively. A programmable acoustic wave disrupted the compound (core/annulus) jet into nascent core/shell droplets. Materials, solvent concentrations, and surfactants were modulated to determine conditions producing a uniform shell surrounding the liquid core. In addition, the phase separation of core and shell materials was evaluated as well as the localization of fluorescent molecular probes. Ultimately, the distinct phase separation of an aqueous core loaded with bovine serum albumin resulted in pulsed release upon sufficient degradation of the PLGA shell.

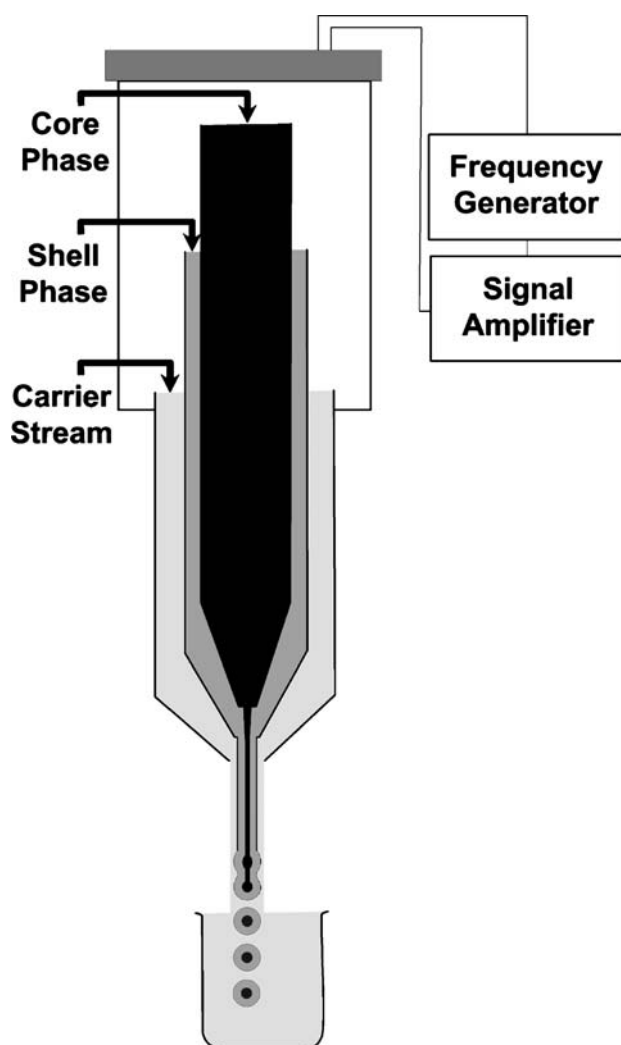


Fig. 1. Schematic diagram of the PPF apparatus.

MATERIALS AND METHODS

Materials. Different 50:50 poly-(D,L-lactide-co-glycolide) (M_w ranging from $\sim 10,000$ to $65,000$) were supplied by Absorbable Polymers. Poly(1,6-bis-*p*-carboxyphenoxyhexane) was generously provided by Dr. Balaji Narasimhan from the Department of Chemical Engineering at Iowa State University. Polilactofate[®] and 20:80 poly(1,6-bis-*p*-carboxyphenoxypropane-co-sebacic anhydride) were generously donated by Guilford Pharmaceuticals. Polyvinyl alcohol was provided by Polysciences, Inc. Rhodamine B base and bovine serum albumin were attained from Sigma. Nile red and sulforhodamine B were purchased from Molecular Probes. Silicone oil (20 cP) and analytical grade dichloromethane were acquired from Fisher Scientific. Fluorescein isothiocyanate-dextran (F-Dex, $M_w \sim 70,000$) was purchased from Sigma.

Labeling of Bovine Serum Albumin. Approximately 500 mg of BSA was added to 100 mL of phosphate buffered saline solution (PBS, pH = 7.4) that contained 840.39 mg of sodium bicarbonate resulting in a solution pH of 8.95. Nine mg of sulforhodamine B acid chloride was mixed with 200 μL of DMF and this dye solution was added to the protein solution, which was mixed for 2 h at 37°C . The reaction was stopped by the addition of 1.5 M hydroxylamine and incubating for an additional hour. To remove unbound dye, the solution was placed in an ultrafiltration column (Millipore Centrplus YM-10, molecular weight cut-off 100 kDa) and centrifuged at $3,000 \times g$ for four 30-min periods, refreshing the column and retained R-BSA with nanopure water each period. The resulting concentrated, labeled and salt-free protein solution was lyophilized and stored at -20°C in the dark, under desiccant.

Generation of Uniform Microcapsules. A coaxial nozzle design was employed to create a compound core/annular jet surrounded by an aqueous jet containing 0.5% polyvinyl alcohol as a stabilizing agent. The volumetric flow-rates of the syringe pump driven jets were systematically varied so as to encourage the formation of a compound laminar jet of the desired diameter, which was subsequently disrupted into uniform core/shell droplets via an acoustic wave excitation generated by a piezoelectric transducer driven by an amplified (Trek PZD700) sinusoidal signal (Agilent 33120A) and tuned to the required frequency. The jets flowed into a beaker containing approximately 900 mL of 0.5% PVA. Nascent polymer drops were stirred for approximately 3 h, filtered, and rinsed with an equal volume of distilled water to remove residual PVA. Finally, microspheres were either freeze-dried (Labconco benchtop model) for 2 days and stored at -20°C under desiccant or immediately imaged. Polymer concentrations ranged from 3–50% w/v solvent, typically dichloromethane for these studies. In some cases, rhodamine B base, nile red, or sulforhodamine B-labeled BSA were dissolved in the appropriate solution to visualize the core and shell and to study molecular partitioning within the formed microcapsules.

In Vitro Drug Release. Approximately 25 mg of microspheres were weighed into glass vials and 2 mL of PBS containing 0.005% Tween 20 were added to each vial. The samples were incubated at 37°C while shaking at 225 revolutions per minute. One mL of supernatant was removed at selected time points and replaced with fresh buffer. The

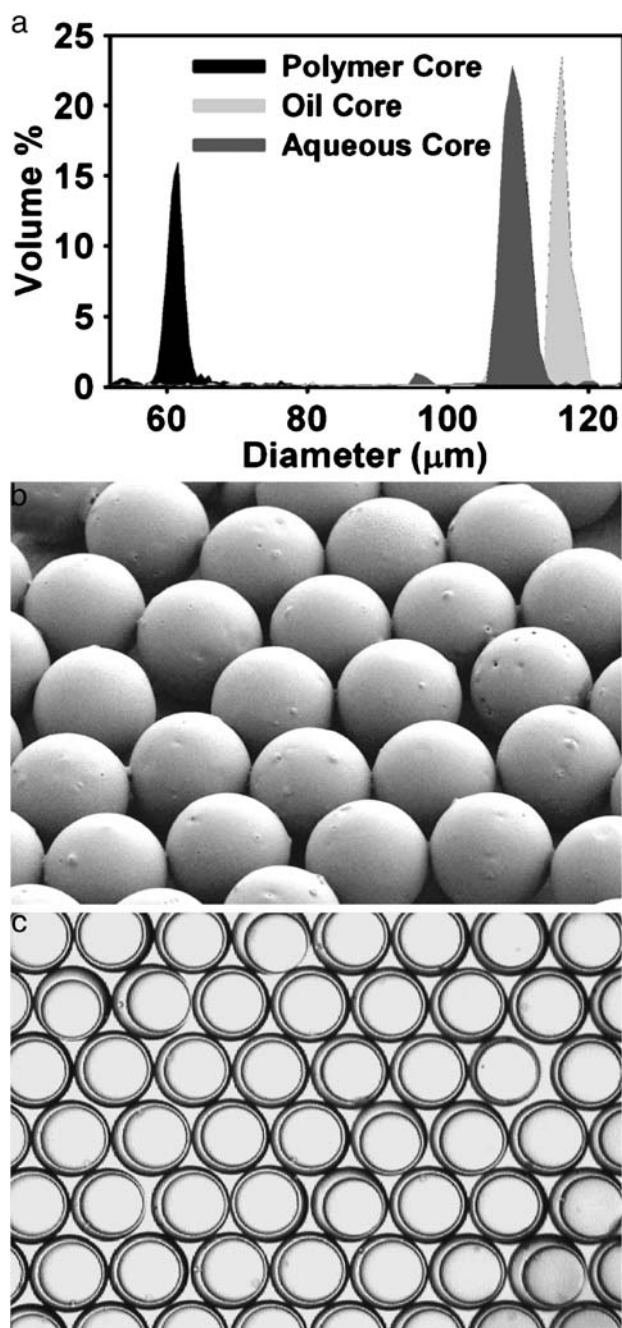


Fig. 2. (a) Coulter Multisizer size distributions for different polymer, oil, and aqueous core microcapsules (see details in text). (b) Scanning electron micrograph depicting the uniformity and surface morphology of ~ 115 μm canola oil core/PLG shell microcapsules (oil core not visible). (c) Optical micrograph of ~ 110 μm microcapsules encapsulating an aqueous core containing 100 mg/mL dextran and 10 mg/mL BSA with a PLG shell.

concentration of fluorescein isothiocyanate-labeled dextran or sulforhodamine B-labeled BSA in the supernatant for each time point was determined using an excitation wavelength of 491 nm and emission wavelength of 513 or 560 nm and 578 nm, respectively. The release data were summed for each time point, and the total divided by the actual drug loading to arrive at the cumulative percent released. The encapsulation efficiency of each molecule was $\sim 100\%$.

Microcapsule Characterization. A Coulter Multisizer III determined the size distribution of the various microcapsule formulations. Optical and laser scanning confocal micrographs were acquired using an Olympus Fluoview FV300 Laser Scanning Biological Microscope. Rhodamine B, Nile red, and sulforhodamine B were excited with a krypton laser (~ 568 nm).

RESULTS

Coulter Multisizer size distributions indicated that monodisperse microcapsules were produced from a variety of materials including; a poly(D,L-lactide-co-glycolide) (PLG) core with poly(1,6-bis-*p*-carboxyphenoxyhexane) (PCPH) (25) shell, a silicone oil core with PLG shell, and an aqueous core containing 100 mg/mL dextran and 10 mg/mL bovine serum albumin (BSA) with PLG shell (Fig. 2a). In each case, $>90\%$ of the particles were within 2 μm of the average diameter. A scanning electron micrograph depicts the uniformity and surface morphology of PLG microcapsules encapsulating the silicone oil core (Fig. 2b) while an optical micrograph reveals the particle uniformity of the aqueous core microcapsules (Fig. 2c).

Fabrication conditions were investigated to control shell thickness and the uniformity of thickness. Utilizing canola oil as the core jet and a 5% w/v solution of PLG in dichloromethane as the annular jet, the relative volumetric flow-rates of the two streams were modulated. Steadily increasing the canola oil flow-rate while maintaining a constant PLG solution

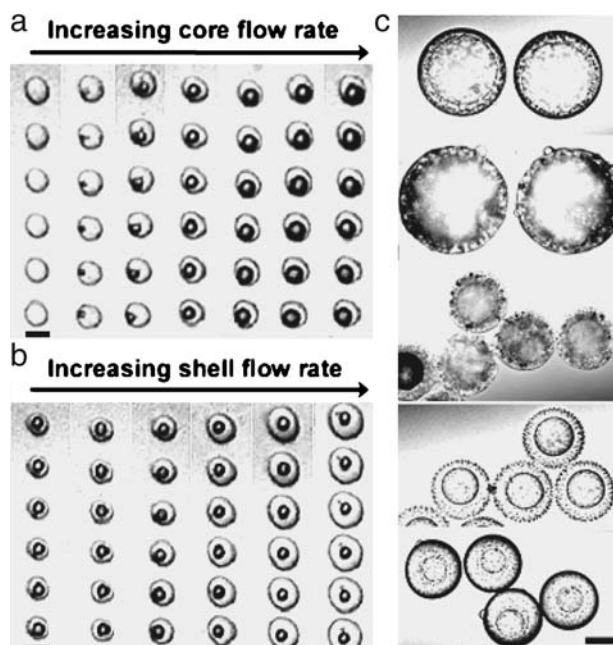


Fig. 3. At a constant acoustic excitation frequency, photomicrographs depict the effect of increasing the flow rate of (a) the canola oil core phase or (b) PLG in dichloromethane annular phase. Scale bar = 100 μm . (c) Various materials were utilized to illustrate control of the final hardened shell thickness and overall microcapsule diameter (from top to bottom: silicone oil in Polilactofate[®], canola oil in PLG, canola oil in poly(1,6-bis-*p*-carboxyphenoxypropane-*co*-sebacic anhydride), and silicone oil in thin and thick PLG shells). Scale bar = 25 μm .

flow-rate and acoustic excitation (break-up) frequency resulted in a steadily increasing core diameter, as expected (Fig. 3a). The growth of the canola oil droplet within the PLG/dichloromethane droplet was significant, increasing from 0 to >60 μm in diameter and producing a 25% increase in overall droplet diameter. Increasing the shell PLG solution

volumetric flow-rate by several fold while holding the oil flow-rate constant resulted in an increasing volume of shell material while maintaining a constant core diameter (Fig. 3b). The ability to steadily increase the thickness of a polymer shell was exemplified in a variety of oil core/polymer shell combinations including (from top to bottom Fig. 3c) silicone

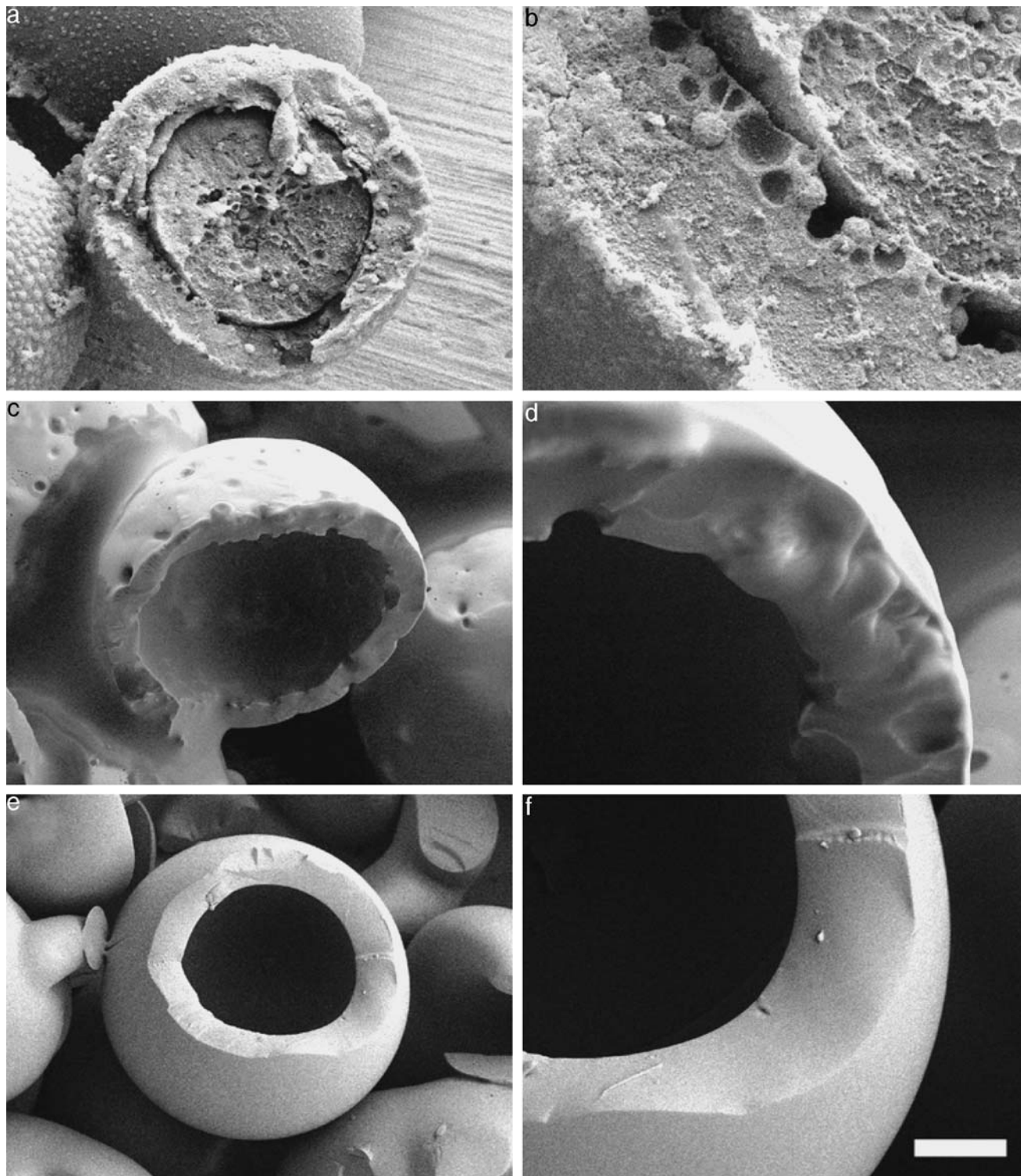


Fig. 4. Scanning electron micrographs showing the interfacial interactions of (a) and (b) a PCPH core/PLG shell microcapsule, (c) and (d) a canola oil core/PLG shell microcapsule, and (e) and (f) a 100 mg/mL dextran plus 10 mg/mL BSA loaded aqueous core/PLG shell microcapsule. Scale bar = (a) 10 μm , (b) 2 μm , (c) 25 μm , (d) 6 μm , (e) 33 μm , and (f) 11 μm .

oil in Polylactofate[®], canola oil in PLG, canola oil in poly(1,6-bis-*p*-carboxyphenoxyhexane-*co*-sebacic anhydride) (PCPH-*co*-SA), and silicone oil in thin and thick PLG shells.

Investigating the localization of core and shell phase materials revealed that discrete intermingling of phases often occurred at the interface of materials. Scanning electron micrographs of cross-sectioned microcapsule formulations indicated some mixing of “like” phases (e.g., polymer/polymer, oil/polymer) across the boundary separating the core and shell. In the case of microcapsules exhibiting a PCPH core encapsulated by a PLG shell, a distinct boundary between the two polymer phases seemed evident; however, higher magnification of the polymer interface as well as at the particle outer

surface revealed microphase separation indicating the presence of both polymers (Fig. 4a and b). Selective dissolution of PLG in these microcapsules or “double-walled” microspheres confirmed the position of PLG as the core phase (16). This phenomenon is also evident in an oil core as canola oil breached into a PLG shell and created small but unconnected pores at the microcapsule surface (Fig. 4c and d). However, microcapsules encapsulating a solution of 100 mg/mL dextran plus 10 mg/mL BSA in water showed a dense shell with negligible intrusion of the core phase due to minimal core/shell miscibility (Fig. 4e and f).

Of particular interest in controlled release is the ability to isolate molecules to specific regions of the particle. PPF

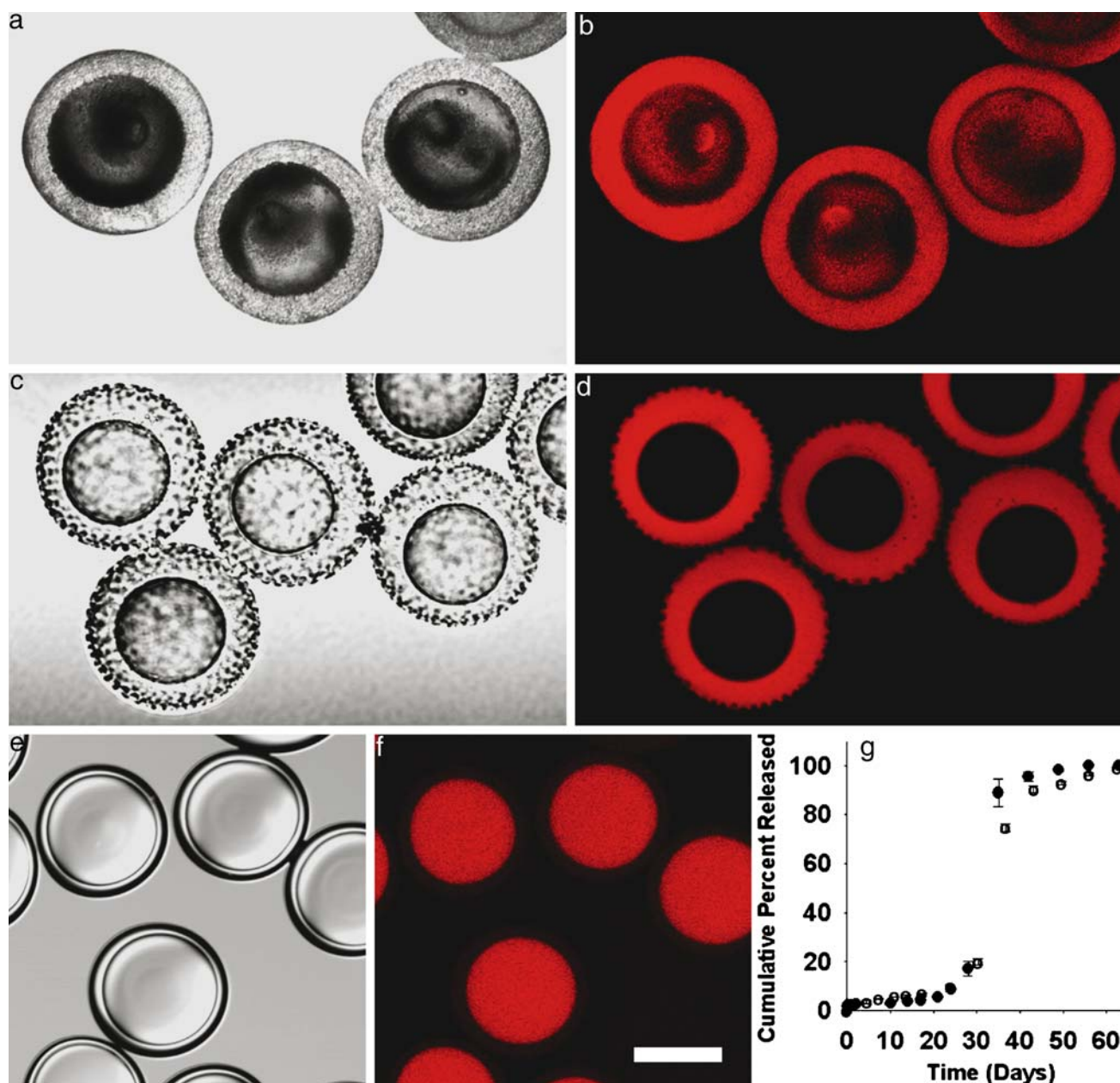


Fig. 5. Optical and laser scanning confocal micrographs revealing the distribution of (a) and (b) rhodamine B base in PLG core/PCPH shell microcapsules localized to the shell phase, (c) and (d) Nile red in silicone oil core/PLG shell microcapsules localized to the shell phase, and (e) and (f) sulforhodamine B-labeled BSA in aqueous core/PLG shell microcapsules localized to the core phase. (g) 30-day pulsatile release of dextran (closed circles) or BSA (open circles) from distinct formulations. Scale bar = 25 μ m for (a),(b),(c),(d) and 75 μ m for (e),(f).

embodies an ability to incorporate a given molecule into the specific phase of interest prior to microcapsule fabrication. Depending on the relative partitioning of the molecule and the solvent extraction (hardening) rate, the compound of interest can be localized to the specified core or shell phase (19,26,27). In the case of a PLG core encapsulated by a PCPH shell, rhodamine B base was retained preferentially in the shell phase even though the polymer phases are quite similar and were dissolved in a common solvent, dichloromethane, prior to particle formation (Fig. 5a and b). Interestingly, microcapsule systems with minimal miscibility between core and shell phases that encapsulate molecules with a strong preference for a particular phase reveal near 100% localization of the encapsulated molecule to either the polymer shell or the core phase. For example, the dye Nile red did not partition into the silicone oil core but remained in the PLG shell (Fig. 5c and d). Similarly, sulforhodamine B-labeled BSA was retained in the aqueous core phase and excluded from the PLG shell (Fig. 5e and f). Leveraging spatial control of molecule localization allowed pulsatile release profiles of dextran and BSA from PLG microcapsules (diameter $\sim 110 \mu\text{m}$; shell thickness $\sim 8 \mu\text{m}$; Mw $\sim 15,000 \text{ Da}$) after a lag phase where minimal release occurred (Fig. 5g). Presumably, varying the polymer shell thickness or material would modulate the duration of the lag phase. Multiple “pulses” from admixed formulations may be attainable, similar to the strategy of “microwells” on a chip (28), but in a facile injection instead of an implant.

DISCUSSION

Several theories are of paramount importance for understanding microcapsule formation. Lord Rayleigh’s theory for predicting jet break-up and droplet size has been reported in detail previously (8,15,23). Microcapsule core and overall radius are predicted according to the disruption of a cylindrical element of the compound jet by a standing acoustic wave of wavelength, λ , according to the equation;

$$r_d = \left(3r_j^2 v_j / 4f\right)^{1/3} \quad (1)$$

where r_d is the drop radius, r_j is the jet radius, v_j is the jet velocity, and f is the wave frequency ($f = v_j / \lambda$). This theory assumes complete immiscibility of the three phases over a working range of $7r_j < \lambda < 36r_j$. In the formed droplets, interfacial tension between the three phases may be used for predicting the spreading coefficient according to;

$$\lambda_{ij} = \gamma_{jk} - \gamma_{ij} - \gamma_{ik} \quad (2)$$

where λ_{ij} is the spreading coefficient and γ_{ij} is the interfacial tension between the denoted phases (19,24). The spreading coefficient may be varied by changing polymer solvent and/or concentration, aqueous surfactant, etc (19). Finally, encapsulating an aqueous core requires carefully balancing core osmolarity with the osmolarity of the aqueous extraction phase. An imbalance in osmotic pressure may promote transfer of water into or out of the core resulting in microcapsule rupture.

CONCLUSIONS

Modified PPF technology represents a single-step method for producing uniform, liquid-core microcapsules of controllable size and shell thickness. Modulating the locale of molecules of interest requires knowledge of droplet formation and dynamic phase separation mechanisms. Oil and aqueous cores encapsulated within uniform polymeric shells offer the potential for pulsed delivery of drugs or vaccines. Finally, PPF production of monodisperse microcapsules possesses industrially relevant advantages in reproducibility, scalability, and consistency of physicochemical properties of microencapsulated products.

ACKNOWLEDGMENTS

Scanning electron micrographs were attained at the Center for Microanalysis of Materials, University of Illinois, which is partially supported by the U.S. Department of Energy under grant DEFG02-91-ER45439. Special thanks to Dr. Balaji Narasimhan for providing polyanhydrides and to Guilford Pharmaceuticals for the gift of Polilactofate[®].

REFERENCES

1. L. Zha, Y. Zhang, W. Yang, and S. Fu. Monodisperse temperature-sensitive microcontainers. *Adv. Mater.* **14**:1090–1092 (2002).
2. A. Sanchez, R. K. Gupta, M. J. Alonso, G. R. Siber, and R. Langer. Pulsed controlled-release system for potential use in vaccine delivery. *J. Pharm. Sci.* **85**:547–552 (1996).
3. C. Berkland, M. King, A. Cox, K. Kim, and D. Pack. Precise control of PLG microsphere size provides enhanced control of drug release rate. *J. Control. Release* **82**:137–147 (2002).
4. C. Berkland, M. Kipper, K. Kim, B. Narasimhan, and D. Pack. Microsphere size, precipitation kinetics, and drug distribution control drug release from biodegradable polyanhydride microspheres. *J. Control. Release* **94**:129–141 (2003).
5. J. H. Moon, G. R. Yi, S. Yang, D. J. Pine, and S. B. Park. Electrospray-assisted fabrication of uniform photonic balls. *Adv. Mater.* **16**:605–609 (2004).
6. S. M. Chia, *et al.* Multi-layered microcapsules for cell encapsulation. *Biomaterials* **23**:849–856 (2002).
7. C. Chen, M. Chen, T. Serizawa, and M. Akashi. *In situ* formation of silver nanoparticles on poly(N-isopropylacrylamide)-coated polystyrene microspheres. *Adv. Mater.* **10**:1122–1125 (1998).
8. L. Martin-Banderas, *et al.* Towards high-throughput production of uniformly encoded microparticles. *Adv. Mater.* **18**:559–564 (2005).
9. S. Takeuchi, P. Garstecki, D. B. Weibel, and G. M. Whitesides. An axisymmetric flow-focusing microfluidic device. *Adv. Mater.* **17**:1067–1073 (2005).
10. C. Berkland, D. W. Pack, and K. Kim. Controlling surface nanostructure using flow-limited field-injection electrostatic spraying (FFESS) of poly(D,L-lactide-co-glycolide). *Biomaterials* **25**:5649–5658 (2004).
11. I. G. Loscertales, *et al.* Micro/nano encapsulation via electrified coaxial liquid jets. *Science* **295**:1695–1698 (2002).
12. Y. Zhang, Y. Guan, S. Yang, J. Xu, and C. C. Han. Fabrication of hollow capsule based on hydrogen bonding. *Adv. Mater.* **15**:832–835 (2003).
13. M. Zhang, G. Gao, C.-Q. Li, and F.-Q. Liu. Titania-coated polystyrene hybrid micro-balls prepared with miniemulsion polymerization. *Langmuir* **20**:1420–1424 (2004).
14. C. Berkland, K. Kim, and D. W. Pack. PLG microsphere size controls drug release rate through several competing factors. *Pharm. Res.* **20**:1055–1062 (2003).

15. C. Berkland, K. Kim, and D. W. Pack. Fabrication of PLG microspheres with precisely controlled and monodisperse size distributions. *J. Control. Release* **73**:59–74 (2001).
16. C. Berkland, E. Pollauf, D. W. Pack, and K. K. Kim. Uniform double-walled polymer microspheres of controllable shell thickness. *J. Control. Release* **96**:101–111 (2004).
17. E. J. Pollauf, C. Berkland, K. K. Kim, and D. W. Pack. *In vitro* degradation of polyanhydride/polyester core-shell double-wall microspheres. *Int. J. Pharm.* **301**:294–303 (2005).
18. E. J. Pollauf, K. K. Kim, and D. W. Pack. Small-molecule release from poly(D,L-lactide)/poly(D,L-lactide-co-glycolide) composite microparticles. *J. Pharm. Sci.* **94**:2013–2022 (2005).
19. E. J. Pollauf and D. W. Pack. Use of thermodynamic parameters for design of double-walled microsphere fabrication methods. *Biomaterials* **27**:2898–2906 (2006).
20. J. L. Guttman, C. D. Hendricks, K. Kim, and R. J. Turnbull. An investigation of the effects of system parameters on the production of hollow hydrogen droplets. *J. Appl. Phys.* **50**:4139–4142 (1979).
21. K. Kim, K. Y. Jang, and R. S. Upadhye. Hollow silica spheres of controlled size and porosity by sol–gel processing. *J. Am. Ceram. Soc.* **74**:1987–1992 (1991).
22. N. K. Kim, K. Kim, D. A. Payne, and R. S. Upadhye. Fabrication of hollow silica aerogel spheres by a droplet generation method and sol–gel processing. *J. Vac. Sci. Technol. A* **7**:1181–1184 (1989).
23. L. Rayleigh. *Proc. Lond. Math. Soc.* **10**:4 (1879).
24. K. J. Pekarek, J. S. Jacob, and E. Mathiowitz. One-step preparation of double-walled microspheres. *Adv. Mater.* **6**:684–687 (1994).
25. M. J. Kipper, E. Shen, A. Determan, and B. Narasimhan. Design of an injectable system based on bioerodible polyanhydride microspheres for sustained drug delivery. *Biomaterials* **23**:4405–4412 (2002).
26. N. A. Rahman and E. Mathiowitz. Localization of bovine serum albumin in double-walled microspheres. *J. Control. Release* **94**:163–175 (2004).
27. M. Shi, *et al.* Double walled POE/PLGA microspheres: encapsulation of water-soluble and water-insoluble proteins and their release properties. *J. Control. Release* **89**:167–177 (2003).
28. A. C. Richards Grayson, *et al.* Multi-pulse drug delivery from a resorbable polymeric microchip device. *Nat. Mater.* **2**:767–772 (2003).